

Enhancement of the crystalline phase in poly(vinylidene fluoride) by using the electrospinning technique and graphene oxide composition

Nguyen Thi Thu Thuy^{1,*}, Vu Ngọc Phan², Trinh Thi Hai³



Use your smartphone to scan this QR code and download this article

¹Phenikaa University Nano Institute, Phenikaa University, Ha Dong district, Hanoi, Vietnam

²Faculty of Biological, Chemical and Environmental Engineering, Phenikaa University, Ha Dong district, Hanoi, Vietnam

³Faculty of Chemical Engineering, Hanoi University of Industry, Bac Tu Liem District, Hanoi, Vietnam

Correspondence

Nguyen Thi Thu Thuy, Phenikaa University Nano Institute, Phenikaa University, Ha Dong district, Hanoi, Vietnam

Email: thuy.nguyenthithu@phenikaa-uni.edu.vn

History

- Received: 2023-02-20
- Accepted: 2023-05-23
- Published: 2023-06-30

DOI :

<https://doi.org/10.32508/stdj.v26i2.4048>



Copyright

© VNUHCM Press. This is an open-access article distributed under the terms of the Creative Commons Attribution 4.0 International license.



ABSTRACT

Introduction: Poly(vinylidene fluoride) (PVDF) possesses some unique characteristics, such as piezoelectric, ferroelectric, and pyroelectric properties. The β crystalline phase of PVDF exhibits the strongest piezoelectric and pyroelectric properties. In this study, the influence of the electrospinning process and graphene oxide (GO) composition on the β -phase formation of PVDF fibers is reported. **Methods:** The morphology of electrospun PVDF and PVDF/GO fibers was observed using a scanning electron microscope (SEM). Characteristics of the crystal phase of electrospun PVDF and PVDF/GO fibers were analyzed by Fourier transform infrared spectroscopy (FTIR), Raman spectroscopy, X-ray diffraction (XRD), and differential scanning calorimetry (DSC). **Results:** The PVDF fiber fabricated by the electrospinning technique had a crystallinity degree that increased by more than 117% compared to that of the precursor PVDF powder. The X-ray diffraction results show that the entire α phase of PVDF was converted to the β phase due to elongation deformation under the force of an electrical field during the electrospinning process. The presence of GO also induced the formation of the β phase of PVDF due to the interaction between the atomic groups on the surface of GO sheets and on the PVDF molecular chains. **Conclusion:** Both the electrospinning process and GO led to an increase in the crystallinity of PVDF. PVDF/GO nanofibers with crystallinity degrees above 60% can be applied in many fields, such as water purification membranes, air filters, energy harvesting materials, biosensors, and catalysts.

Key words: electrospinning, polyvinylidene fluoride, polymer nanofibers, crystalline phase, piezoelectric materials

INTRODUCTION

Poly(vinylidene fluoride) (PVDF) is widely used in various applications due to its excellent mechanical strength, chemical resistance, and some unique properties, such as piezoelectricity, ferroelectricity, and thermoelectricity¹. PVDF is a semicrystalline homopolymer that is made up of monomer units ($-\text{CH}_2-\text{CH}_2-$). PVDF has five crystallite polymorphs, including α , β , γ , δ , and ϵ phases². Each phase imparts specific properties to the polymer and therefore has distinct applications. The α phase exhibits better thermodynamic stability. Meanwhile, the β phase shows the strongest piezoelectric and thermoelectric properties³. In the α -phase conformation, the average dipole moment per monomer is decreased because the dipole is tilted relative to the normal axis. Moreover, the lattice of the α -phase comprises two molecular chains in a trans conformation, whose dipole components are antiparallel to the chain axis and mutually neutral. As a result, the α phase is nonpolar and does not display piezoelectric and thermoelectric properties. The β -phase conformation

has dipoles that are parallel to the chain axis thus, this conformation induces large spontaneous polarization and displays strong ferroelectric and piezoelectric properties^{4,5}. Because of these unique properties of the β -phase, PVDF has been applied in the manufacture of actuators, biosensors, energy harvesting devices, filtration membranes, etc. For liquid and gas filtration, piezoelectric PVDF membranes can reduce fouling by preventing the deposition of filtrate on the membrane surface. As a piezoelectric material, PVDF has the ability to convert mechanical strain into electrical energy, which is used in energy harvesting devices^{6,7}.

The β -phase of PVDF can be formed by conversion from the α -phase by using techniques such as mechanical drawing and electrical poling⁸. Electrospinning, a technique to fabricate nanofibers, is considered an effective method to cause the crystal phase transition of polymeric materials. In the electrospinning process, the polymer solution is stretched into nanofibers by the force of the electric field during its travel from the needle tip to the collector (Figure 1).

Cite this article : Thuy N T T, Phan V N, Hai T T. **Enhancement of the crystalline phase in poly(vinylidene fluoride) by using the electrospinning technique and graphene oxide composition.** *Sci. Tech. Dev. J.* 2023; 26(2):2741-2747.

Thus, electrospinning causes uniaxial elongation of the PVDF molecular chains along the fiber axis, leading to the formation of the β -phase⁸. Some studies have reported that the β -phase content of electrospun PVDF nanofibers is strongly influenced by various parameters of the electrospinning process, including solution parameters (solution concentration, solvent system, molecular weight), processing variables (applied voltage, spinning distance, flow rate, fiber collector), and environmental conditions (temperature and humidity)⁹. To enhance the piezoelectricity of electrospun PVDF fibers for energy harvesting, Szewczyk *et al.*¹⁰ investigated the effect of voltage polarity and environmental humidity on the electrospinning of PVDF. The authors reported that a two times higher composition of the β -phase was obtained at a humidity of 60% compared to 30%. The solvent system is one of the factors affecting not only the morphology but also the crystal structure of the electrospun PVDF nanofibers. The solution containing a high fraction of a low volatile solvent crystallizes slowly, providing enough time to nucleate the thermodynamically stable β -phase⁹. In addition, the preparation of electrospun PVDF nanofibers with the incorporation of nanofillers, such as metal oxides^{9,11}, carbon nanotubes¹², graphene¹³, and GO¹⁴, could facilitate β -phase formation. For example, the piezoelectricity of PVDF nanofibers was enhanced by adding graphene as a nanofiller due to the interaction between the π bonds of graphene and fluorine atoms in PVDF inducing the formation of the β -phase¹³. It has been reported that incorporating fillers containing carbonyl groups into the PVDF matrix resulted in their homogeneous dispersion and enhanced the β -phase of PVDF. Similarly, GO showed high compatibility with PVDF because of the strong interaction between carbonyl groups appearing on the GO surface and the fluoride group of PVDF and resulted in the formation of the pure β -phase of GO/PVDF nanocomposite films^{15,16}.

This study analyzed and evaluated the formation of the β -phase due to two impact factors: the influence of the electrospinning process and the influence of the presence of graphene oxide (GO). The morphology and phase characteristics of the materials were analyzed by several analytical methods: scanning electron microscopy (SEM), infrared spectroscopy (IR), X-ray diffraction (XRD), Raman spectroscopy, and differential scanning thermal (DSC).

MATERIALS AND METHOD

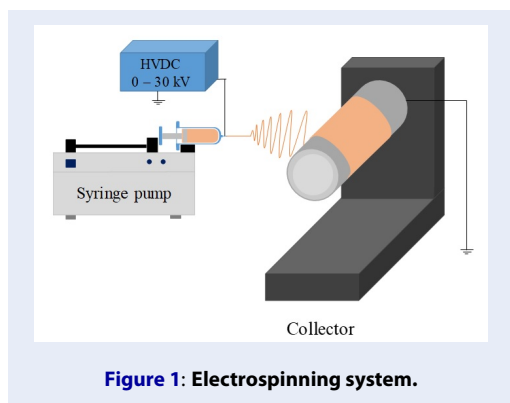


Figure 1: Electrospinning system.

Materials

Graphite flake (99% carbon, from 50-800 μm in diameter and 1-150 μm thick, Sigma Aldrich); H_2SO_4 (96%, China), H_2O_2 (30%, China); HCl (China); KMnO_4 (99.5%, Vietnam); PVDF powder (Kynar@761A), *N,N*-dimethylacetamide (DMAc \geq 99.0%, Sigma Aldrich) and acetone (\geq 99.7%, Sigma Aldrich).

Method

GO was prepared from graphite flakes by the modified Hummer method as reported in our previous study¹⁷. Briefly, 3 g of graphite powder was put in a 500 ml flask placed in an ice bath. Then, 45 ml of concentrated H_2SO_4 was added and stirred for 30 minutes. Next, 0.45 g of KMnO_4 was slowly added to the above mixture and stirred for 15 minutes. Then, 9.0 g of KMnO_4 was continuously added so that the temperature of the mixture did not exceed 90 $^\circ\text{C}$. The mixture was stirred at 90 $^\circ\text{C}$ for 1 h, and then 120 ml of distilled water was slowly added and stirred for another 20 min. Then, 10.5 ml of H_2O_2 and 80 ml of distilled water were poured into the above mixture. After stirring for 30 minutes, the mixture was filtered to obtain a graphite oxide cake. Graphite oxide was further dispersed in 200 ml of 0.1 M HCl and stirred for 20 min. Then, it was filtered and washed several times with distilled water, dried at 80 $^\circ\text{C}$ for 12 hours, ground, and sifted into graphite oxide powder. Finally, the graphite oxide powder was dispersed in distilled water to reach a concentration of 0.1 mg/ml and exfoliated by a tip sonicator (MW-2000, SINEO) for 10 min to obtain GO.

A 14 wt% PVDF solution for the electrospinning process was prepared by dissolving 1.4 g PVDF in a mixed solvent of 5.16 g DMAc and 3.44 g acetone using a magnetic stirrer at 60 $^\circ\text{C}$. To prepare a 14 wt% PVDF solution containing 4 wt% GO (PVDF/GO4), 0.056

g GO was dispersed into a mixture solvent of 5.16 g DMAc and 3.44 g acetone in an ultrasonic bath for 1 hour. Next, 1.4 g PVDF was added into the above mixture and stirred at a temperature of 60 °C.

Electrospun PVDF fibers were fabricated by the following steps. PVDF solution was filled into a 5 mL syringe with a stainless-steel needle. The syringe was placed on a microinfusion pump, and the feed rate of the solution was set at 1.0 mL/h. The voltage applied to the needle was 10 kV. The distance between the needle and the collector was 20 cm, and the rotating speed of the collector was 800 rpm.

The morphology of PVDF and PVDF/GO fibers was observed by SEM (JSM-6510LV). The characteristics of the fibers were analyzed by an FTIR spectrophotometer (NEXUS 670 from Nicolet), a Raman spectrometer (MacroRAM, Horiba), and X-ray diffractometers (XRD EQUINOX 5000).

RESULTS

SEM images of PVDF and PVDF/GO fiber membranes fabricated by the electrospinning technique are shown in Figure 2. The PVDF fibers had a uniform morphology with an average diameter of 2717 ± 314 nm. Its distribution of fiber diameter was narrow. The average diameter of PVDF/GO4 fibers was 3085 ± 610 nm, with a wider fiber diameter distribution compared with that of PVDF fibers.

FTIR spectra of PVDF powder, electrospun PVDF fibers, and electrospun PVDF/GO fibers between 600 and 1000 cm^{-1} are displayed in Figure 3. In the case of the PVDF powder, the characteristic peaks of the α phase appeared at 613 cm^{-1} , 763 cm^{-1} , 796 cm^{-1} , and 974 cm^{-1} corresponding to the vibrations of skeletal bending, CF_2 bending, CH_2 rocking, and CH_2 twisting, respectively. In addition, it has a weak peak at 840 cm^{-1} (CH_2 rocking), which is a signal of the β phase¹⁸. In the FTIR spectra of electrospun PVDF and PVDF/GO fibers, the intensity of the peak attributed to the β phase at 840 cm^{-1} increased, while other peaks characterizing the α phase disappeared.

Figure 4 presents the XRD patterns of GO, PVDF powder, PVDF fibers, and PVDF/GO4 fibers fabricated by the electrospinning technique. In the XRD pattern of GO, a peak appeared at 10.6° corresponding to the interlayer spacing between graphitic sheets. The XRD pattern of PVDF powder shows peaks at diffraction angles of 18.7° , 26.7° , and 39.3° , which are typical for the reflection of the crystal planes (020), (021), and (002), respectively. These were characteristic peaks for the α phase of PVDF crystals. The crystal structure of the β phase is characterized by a high-intensity peak at 20.4° and a weak intensity

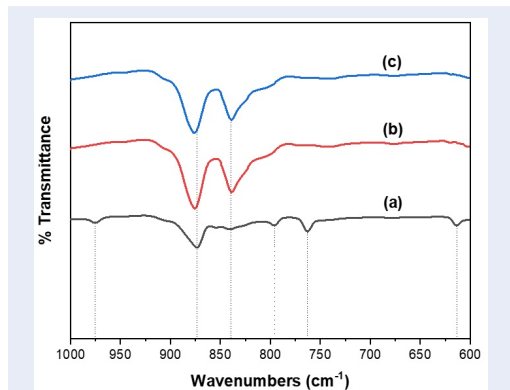


Figure 3: FTIR spectra of (a) PVDF powder, (b) electrospun PVDF fibers, and (c) electrospun PVDF/GO4 fibers.

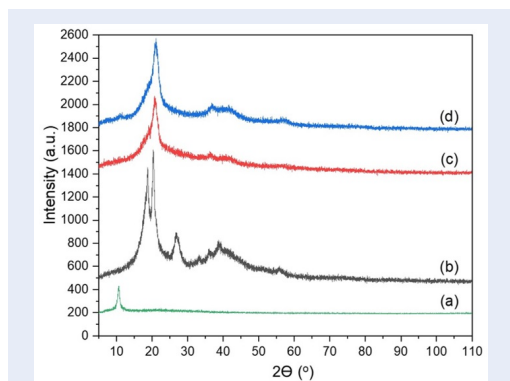


Figure 4: XRD patterns of (a) GO, (b) PVDF powder, (c) electrospun PVDF fibers, and (d) electrospun PVDF/GO4 fibers.

peak at 37.9° , corresponding to the reflection of the (110)/(200) and (020)/(310) planes⁵. In the XRD pattern of the electrospun PVDF fiber membrane, there were two peaks representing the β phase at 20.7° and 37.0° , while the characteristic peaks of the α phase were not observed.

Figure 5 shows the Raman spectra of GO, electrospun PVDF fibers, and electrospun PVDF/GO fibers. The Raman spectrum of GO exhibited D and G bands at wavenumbers of 1312 cm^{-1} and 1594 cm^{-1} , respectively. For electrospun PVDF/GO4, the D band of GO shifted to a lower wavenumber of 1303 cm^{-1} .

DSC diagrams of PVDF powder, electrospun PVDF fibers, and electrospun PVDF/GO fibers and data obtained from DSC diagrams are presented in Figure 6 and Table 1. The crystallinity degree of the samples is

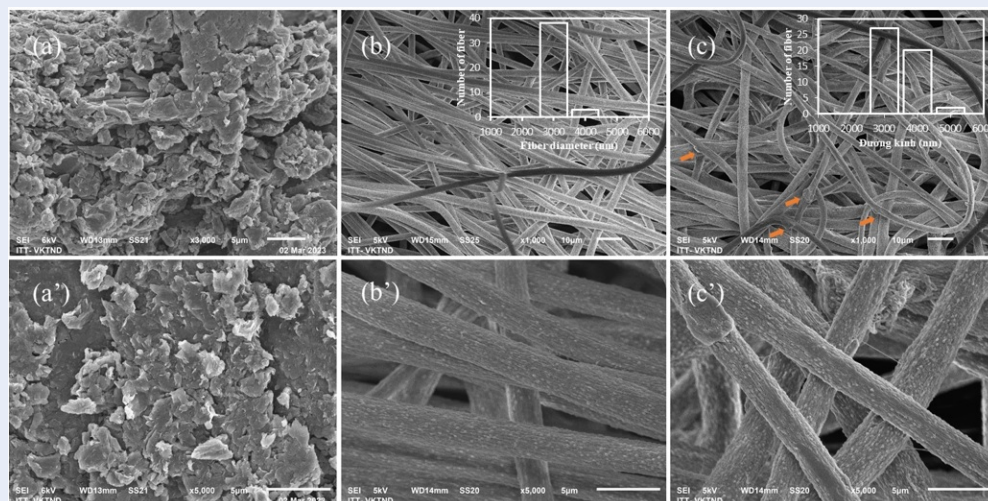


Figure 2: SEM images of GO (a and a'), electrospun PVDF fibers (b and b'), and electrospun PVDF/GO4 fibers (c and c'). The distribution of the fiber diameter of electrospun PVDF and PVDF/GO4 fibers is shown in (b) and (c) images, respectively. The inserted arrows in image (c) show the aggregation of GO sheets.

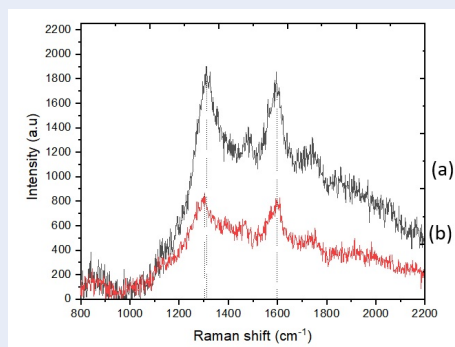


Figure 5: Raman spectra of (a) GO and (b) electrospun PVDF/GO4 fibers.

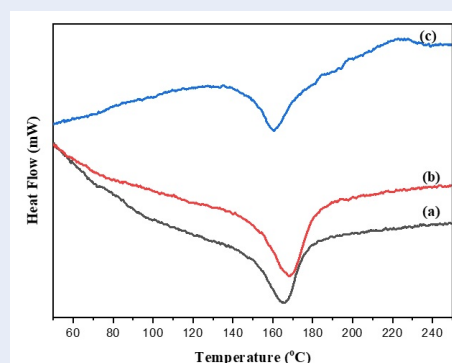


Figure 6: DSC diagrams of (a) PVDF powder, (b) electrospun PVDF fibers, and (c) electrospun PVDF/GO4 fibers.

determined using equation (1) as follows:

$$\%C = \frac{\Delta H_f}{\Delta H_f^0} \times 100\% \quad (1)$$

where ΔH_f^0 is the enthalpy of fusion of 100% crystalline PVDF ($\Delta H_f^0 = 104,7$ J/g) and ΔH_f is the enthalpy of fusion of the samples².

As shown in Table 1, the crystalline degree of the electrospun PVDF fibers (41.86%) was much higher than that of the precursor PVDF powder (19.21%). In addition, the presence of GO also increased the crystalline degree of PVDF from 41.86% to 66.36%.

DISCUSSION

Morphology of electrospun PVDF and PVDF/GO fibers

Electrospun PVDF fibers appeared with uniform morphology. Meanwhile, PVDF/GO fibers occasionally appeared as clusters of particles on the fibers (inserted arrow direction). This might be due to the aggregation of GO sheets into large particles in the PVDF solution. In addition, the diameter of the PVDF/GO4 fibers was larger than that of the PVDF fibers. The presence of GO in the PVDF solution might decrease the charge density of the solution due to the inherent insulating property of GO^{19,20}, resulting in decreased stretching of the polymer jet under electrical force²¹. In addition, the addition of GO in a

Table 1: The melting point (T_m), enthalpy of fusion (ΔH_f), and crystalline degree (%C) of PVDF powder, electrospun PVDF fibers, and electrospun PVDF/GO4 fibers

Samples	T_m ($^{\circ}\text{C}$)	ΔH (J/g)	%C
PVDF powder	164.6	20.11	19.21
PVDF fibers	166.6	43.83	41.86
PVDF/GO4 fibers	159.0	69.48	66.36

polymer matrix also increased the viscosity of the solution^{14,15} consequently, the diameter of PVDF/GO4 increased. Interestingly, the surface of both PVDF and PVDF/GO4 appeared to have a porous structure. This result was caused by the high humidity of the environment (>60%) and the difference in the volatility of DMAc and acetone solvents, leading to phase separation between the inside and outside parts of the solution jet, which was drawn under the electrical field¹⁶.

Influence of the electrospinning process and GO composition on the crystal phase of the PVDF fiber membrane

In the FTIR spectra of electrospun PVDF and PVDF/GO4 fibers, the intensity of the absorption peak of the β phase at 840 cm^{-1} significantly increased, while the characteristic peaks of the α phase at 613 cm^{-1} , 763 cm^{-1} , 796 cm^{-1} , and 974 cm^{-1} completely disappeared¹⁷. Moreover, the bands at 874 cm^{-1} are assigned to C-H wagging²² and the vibration of the β phase²³, which appeared with higher intensity in the FTIR spectra of the electrospun PVDF and PVDF/GO4 fibers than in that of the PVDF powder. These results indicate that the β phase predominated in the electrospun fibers. On the other hand, the electrospinning process and the addition of GO strongly affected the crystal structure of PVDF.

The characteristic peaks of the α phase were not observed in the XRD patterns of the electrospun PVDF and PVDF/GO4 fibers, indicating that the α phase was completely converted into the β phase after the electrospinning process. This is the effect of two factors induced in the electrospinning process: mechanical stretching and electrical poling. Mechanical stretching contributes to the transition of the coiled structure into a crystalline array, in which the molecular chains are arranged into the β -phase conformation. The application of an electrical field on PVDF molecules during the electrospinning process also resulted in the orientation of the crystallite polar axis in the direction of the electrical field, thereby promoting more polarization of the β phase. The addition of GO to the PVDF fiber also affects crystalline phase formation. The electrospun PVDF/GO4

fibers had a complete crystalline form in the β -phase. Moreover, the crystalline degree of the electrospun PVDF/GO4 fibers was higher than that of the electrospun PVDF fibers, as shown by a larger characteristic peak at 20.7° . Interestingly, the diffraction peak of GO disappeared in the XRD pattern of the electrospun PVDF/GO4 fibers. The adsorption of molecular chains of PVDF on the GO sheet surface was completely achieved due to the electrostatic interaction between the functional groups of GO and the dipole groups $-\text{CF}_2$ ²⁴⁻²⁶. When the molecular chains of PVDF adsorbed on the surface of GO lamellae, they became straight, resulting in an ordered structure of the β phase²⁶. Therefore, GO could play the role of a nucleating agent, providing a substrate for PVDF crystal nucleation of the β phase.

The Raman spectrum of GO exhibited D and G bands at wavenumbers of 1312 cm^{-1} and 1594 cm^{-1} , respectively. The D band characterizes the out-of-plane vibration of the defect, and the G band indicates the sp^2 bond vibration in the crystal plane of the GO structure. The D band of GO in the electrospun PVDF/GO fibers shifted to a lower wavenumber, possibly accounting for the interaction between GO and PVDF in the electrospun fibers. The molecular chains of PVDF contain F atoms with a highly electronegative charge. These F atoms could interact with the positively charged C atoms in the carbonyl groups of GO. Hydrogen bonding between the C-H and C-F groups of PVDF and the $-\text{OH}$ and $-\text{COOH}$ groups of GO could also be formed^{24,26}. As a result, GO sheets intercalated between PVDF chains, causing an extension of the α -phase conformation into the β -phase conformation, hence promoting the formation of the β phase.

The crystalline degrees of the precursor PVDF powder, electrospun PVDF and PVDF/GO4 fibers were quantitatively calculated from their enthalpy of fusion obtained by DSC analysis. The crystalline degree of the electrospun PVDF/GO4 fibers was much higher than that of the electrospun PVDF fibers. The crystalline phase of PVDF fibers was formed because the molecular chains of PVDF were arranged and oriented in the direction of the electrical field during the electrospinning process. In addition, the presence

of GO also increased the crystalline degree of PVDF from 41.86% to 66.36%. These data were in agreement with the results obtained by FTIR, XRD, and Raman analysis.

CONCLUSION

This study shows that PVDF and PVDF/GO fiber membranes with a high β phase composition were achieved by using the electrospinning technique and the addition of a GO component. The electrospinning process exerted mechanical stretching and electrical poling in the direction of the electrical field, which completely converted the α phase into the β phase. The degree of crystallinity was significantly increased from 19.21% for the PVDF powder to 41.86% for the electrospun PVDF fibers. GO played the role of nuclei for PVDF crystallization due to the electrostatic interactions between the functional groups of GO and the $-\text{CF}_2$ groups of PVDF, leading to the formation of an ordered structure of the crystal phase. With 4 wt% GO, the crystalline degree of electrospun PVDF/GO4 fibers was 66.36%. Electrospun PVDF/GO fiber membranes with porous structures and high crystallinity can contribute to increasing the performance of materials in many applications, such as water filtration, gas filtration, energy harvesting materials, biosensors, and catalysis.

COMPETING INTERESTS

The authors have no competing interests or personal relationships that could have appeared to influence the work reported in this paper.

ABBREVIATIONS

PVDF: Poly(vinylidene fluoride)
GO: Graphene oxide
SEM: Scanning electron microscope
FTIR: Fourier transform infrared spectroscopy
XRD: X-ray diffraction
DSC: Differential scanning calorimetry
DMAC: N,N-dimethylacetamide

AUTHOR'S CONTRIBUTIONS

Nguyen Thi Thu Thuy and Vu Ngoc Phan designed the experiments and wrote the manuscript. Trinh Thi Hai carried out all experiments.

FUNDING

This research has received funding from the National Foundation for Science and Technology Development (NAFOSTED) in Vietnam in 2019, Grant number 104.02-2019.30.

REFERENCES

- Cozza ES, Monticelli O, Marsano E, Cebe P. On the electrospinning of PVDF: influence of the experimental conditions on the nanofiber properties. *Polym Int.* 2012; 62(1):41-8; Available from: <https://doi.org/10.1002/pi.4314>.
- Costa LMM, Bretas RES, Gregorio RG. Effect of solution concentration on the electrospay/electrospinning transition and on the crystalline phase of PVDF. *Mater Sci Appl.* 2010; 1(4):247-52; Available from: <https://doi.org/10.4236/msa.2010.14036>.
- Gee A, Johnson B, Smith AL. Optimizing electrospinning parameters for piezoelectric PVDF nanofiber membranes. *J Membr Sci.* 2018; 563(1-3):804-12; Available from: <https://doi.org/10.1016/j.memsci.2018.06.050>.
- Moazeni N, Sadrjahani M, Merati AA, Latifi M, Rouhani S. Effect of stimuli-responsive polydiacetylene on the crystallization and mechanical properties of PVDF nanofibers. *Polym Bull.* 2019; 77(7):5373-88; Available from: <https://doi.org/10.1007/s00289-019-03020-6>.
- Lim JY, Kim S, Seo Y. Enhancement of β -phase in PVDF by electrospinning. The 30th international conference of the polymer processing society, AIP conference Proceeding. 2015; 1-5; Available from: <https://doi.org/10.1063/1.4918441>.
- Kim M, Wu YS, Kan EC, Fan J. Breathable and flexible piezoelectric ZnO@PVDF fibrous nanogenerator for wearable applications. *Polymers (Basel).* 2018; 10(7):1-15; Available from: <https://doi.org/10.3390/polym10070745>.
- Prasad G, Liang JW, Zhao W, Yao Y, Tao T, Liang B, Lu SG. Enhancement of solvent uptake in porous PVDF nanofibers derived by a water-mediated electrospinning technique. *J Materomics.* 2021; 7(2):244-53; Available from: <https://doi.org/10.1016/j.jmat.2020.05.004>.
- Ruan L, Yao X, Chang Y, Zhou L, Qin G, Zhang X. Properties and applications of the β phase poly(vinylidene fluoride). *Polymers (Basel).* 2018; 10:228; Available from: <https://doi.org/10.3390/polym10030228>.
- Kalimuldina, G, Turdakyn N, Aby I, Medeubayev A, Nurpeissova A, Adair D, Bakenov Z. A review of piezoelectric PVDF film by electrospinning and its applications. *Sensors.* 2020; 20:5214; Available from: <https://doi.org/10.3390/s20185214>.
- Szewczyk PK, Grady A, Kim SK, Persano L, Marzec M, Krysztal A, Busolo T, Toncelli A, Pisignano D, Bernasik A, Narayan SK, Sajkiewicz P, Stachewicz U. Enhanced piezoelectricity of electrospun polyvinylidene fluoride fibers for energy harvesting. *ACS Appl. Mater. Interfaces.* 2020; 12:13575-13583.
- Han G, Su Y, Feng Y, Lu N. Approaches for increasing the β -phase concentration of electrospun polyvinylidene fluoride (PVDF) nanofibers. *ES Mater Manuf.* 2019; 6:75-80; Available from: <https://doi.org/10.30919/esmm5f612>.
- Cerrada ML, Andres JA, Gonzalez AC, Blazquez EB, Perez E. The β form in PVDF nanocomposites with carbon nanotubes: Structural feature and properties. *Polymers (Basel).* 2023; 15:1491; Available from: <https://doi.org/10.3390/polym15061491>.
- Abolhasani MM, Shirvanimoghaddam K, Naebe M. PVDF/graphene composite nanofibers with enhanced piezoelectric performance for development of robust nanogenerators. *Compos. Sci. Technol.* 2016; 138:49-56; Available from: <https://doi.org/10.1016/j.compscitech.2016.11.017>.
- Abbasipour M, Khajavi R, Yousefi AA, Yazdanshenas ME, Razaighian F, Akbarzadeh A. Improving piezoelectric and pyroelectric properties of electrospun PVDF nanofibers using nanofillers for energy harvesting application. *Polym. Adv. Technol.* 2018; 30:279-291; Available from: <https://doi.org/10.1002/pat.4463>.
- Abbasipour M, Khajavi R, Yousefi AA, Yazdanshenas ME, Razaighian F. The piezoelectric response of electrospun PVDF nanofibers with graphene oxide, graphene, and halloysite nanofillers: a comparative study. *J. Mater. Sci: Mater. Electron.* 2017; 28: 15942-15952; Available from: <https://doi.org/10.1007/s10854-017-7491-4>.

16. Yang J, Zhang Y, Li Y, Wang Z, Wang W, An Q, Tong W. Piezoelectric nanogenerators based on graphene oxide/PVDF electrospun nanofibers with enhanced performances by in situ reduction. *Mater. Today, Commun.* 2021; 26:101629; Available from: <https://doi.org/10.1016/j.mtcomm.2020.101629>.
17. Nguyen TTT, Nguyen HT, Trinh HT, Bui TTT, Le AT, Huy TQ. Effect of the morphological characteristic and composition of electrospun polyvinylidene fluoride/graphene oxide membrane on its Pb²⁺ adsorption capacity. *Macromol. Res.* 2021; 30:124-135; Available from: <https://doi.org/10.1007/s13233-022-0012-1>.
18. Cai A, Lei T, Sung D, Lin L. A critical analysis of the α , β and γ phases in poly(vinylidene fluoride) using FTIR. *RSC Adv.* 2017; 7:15382-89; Available from: <https://doi.org/10.1039/c7ra01267e>.
19. Lin CH, Yeh WT, Chan CH, Lin CC. Influence of graphene oxide on metal-insulator-semiconductor tunneling diodes. *Nanoscale Res Lett.* 2012; 7:343; Available from: <https://doi.org/10.1186/1556-276X-7-343>.
20. Kumar S, Himanshi, Prakash J, Verma A, Suman, Jasrotia R, Kandwal A, Verma R, Godara SK, Khan MAM, Alshehri AM, Ahmed J. A review on properties and environmental applications of graphene and its derivative-based composites. *Catalysts.* 2023; 13:111; Available from: <https://doi.org/10.3390/catal13010111>.
21. Cao X, Chen W, Zhao P, Yang Y, Yu DG. Electrospun porous nanofibers: Pore-forming mechanism and applications for photocatalytic degradation of organic pollutants in wastewater. *Polymers (Basel).* 2022; 14:3990; Available from: <https://doi.org/10.3390/polym14193990>.
22. Daems N, Milis S, Verbeke R, Szymczyk A, Pescarmona PP, Vankelecom IFJ. High-performance membranes with full pH-stability. *RSC Adv.* 2018; 8: 8813-8827; Available from: <https://doi.org/10.1039/C7RA13663C>.
23. Peng Y, Wu P. A two dimensional infrared correlation spectroscopic study on the structure changes of PVDF during the melting process. *Polymer.* 2004; 45: 5295-5299; Available from: <https://doi.org/10.1016/j.polymer.2004.05.034>.
24. Achaby ME, Arrakhiz FZ, Vaudreuil S, Essassi EM, Qaiss A. Piezoelectric β -polymorph formation and properties enhancement in graphene oxide - PVDF nanocomposite films. *Appl. Sur. Sci.* 2012; 258: 7668-7677; Available from: <http://dx.doi.org/10.1016/j.apsusc.2012.04.118>.
25. Lee JE, Eom Y, Shin YE, Hwang AH, Ko HH, Chae HG. Effect of interfacial interaction on the conformational variation of Poly(vinylidene fluoride) (PVDF) chains in PVDF/Graphene oxide (GO) nanocomposition fibers and corresponding mechanical properties. *ACS Appl. Mater. Interfaces.* 2019; 11: 13665-13675; Available from: <https://doi.org/10.1021/acsami.8b22586>.
26. Liu X, Ma J, Wu X, Lin L, Wang X. Polymeric nanofibers with ultrahigh piezoelectricity via self-orientation of nanocrystals. *ACS Nano.* 2017; 11:1901-1910; Available from: <https://doi.org/10.1021/acsnano.6b07961>.